

Home range estimation under a restricted sampling scheme.

Alejandro Cholaquidis^a, Ricardo Fraiman^a, and Manuel Hernandez-Banadik^b

^a Centro de Matemática, Universidad de la República, Uruguay

^b Instituto de Estadística, Universidad de la República, Uruguay

Abstract

The analysis of animal movement has gained attention recently. New continuous-time models and statistical methods have been developed to estimate some sets related to their movements, such as the home-range and the core-area among others, when the information of the trajectory is provided by a GPS. Because data transfer costs and GPS battery life are practical constraints in ecological studies, the experimental designer must make critical sampling decisions in order to maximize information. To capture fine-scale motion, long-term behavior must be sacrificed, and vice versa. To overcome this limitation, we introduce the on–off sampling scheme, where the GPS is alternately on and off. This scheme is already used in practice but with insufficient statistical theoretical support. We prove the consistency of home-range estimators with an underlying reflected diffusion model under this sampling method (in terms of the Hausdorff distance). The same rate of convergence is achieved as in the case where the GPS is always on for the whole experiment. This is illustrated by a simulation study and real data. We also provide estimators of the stationary distribution, its level sets (which give estimators of the core area), and the drift function.

1. Introduction

Home-range was defined by Burt (1943) as “the area traversed by the individual in its normal activities of food gathering, mating, and caring for young.” Its estimation is a major problem in animal ecology. Hence there has arisen a considerable literature on the subject, see for instance the reviews in Worton (1987) or Powell (2000). Another key concept is the so-called core-area (areas where animals spend most of their time); in our setup, core-areas can be modeled by the level sets of the stationary distribution. Several models have been proposed to analyse the home-range as well as the dynamics of animals. The first one (Hayne, 1949) assumed that

the available data are a sequence of locations recorded at some times, and estimates the home-range by means of the convex hull of the points. More flexible proposals have also been introduced, for instance the use of “local convex hulls” (Getz and Wilmers, 2004) or the r -convex hull (Burgman and Fox, 2003), since r -convex sets are a much more flexible class of sets. Some others, referred to as occurrence estimators, are focused on the estimation of the so-called “utilization distribution” (the density function that describes the probability of finding the animal at a particular location). Among these, there is the Brownian bridge model (BBMM), a parametric model introduced in Horne et al. (2007).

The importance of using continuous time models for animal movement is discussed in Kie et al. (2010); Noonan et al. (2019); Fleming et al. (2014, 2015); Calabrese et al. (2016). Home-range estimation is carried out by estimating the support of a density probability function, or an appropriate level set. The importance of taking into account the autocorrelations is deeply analysed in those papers. They reproduce different autocorrelation scenarios (position or velocity autocorrelation) by using continuous-time movement models and contrast a kernel-based home-range estimator designed for iid data, with the autocorrelated kernel density estimation (AKDE), tailored for autocorrelated data (Fleming et al., 2015). Their findings confirm that the first underestimates the home-range, while the latter one performs very well.

AKDE adjusts the smoothing kernel parameter in order to weight properly the contribution of each location point to the estimation of the density: the more dependent the data are, the less ‘new information’ they provide. So, AKDE aims to fit an autocovariance function to compute the estimator. To this end, several animal movement models are proposed, such as the Ornstein–Uhlenbeck, the Ornstein–Uhlenbeck with foraging (Fleming et al., 2014, Supplementary material C), and integrated process are also considered (that ensure velocity autocorrelation), among others (see Noonan et al. (2019); Fleming et al. (2014, 2015); Calabrese et al. (2016)). From a statistical point of view, no asymptotic theory has yet been developed and, more importantly, some of the aforementioned models lack a stationary distribution to be estimated.

From a more theoretical-mathematical point of view, in Cholaquidis et al. (2016) the animal’s motion is modeled as a reflected Brownian motion on a bounded set $S \subset \mathbb{R}^d$ that plays the role of the home-range, and consistent estimators and rates of convergence are obtained. In Cholaquidis

et al. (2021) a reflected Brownian motion with drift is considered (RBMD, see section 2.2), and it is proven that under suitable conditions there exists a unique stationary distribution of the process, and consistent uniform estimators are obtained for the density together with its level sets (that give an estimate of the core-area).

Even though it seems unrealistic to model animal movement with an RBMD, this is mainly due to the good properties of the RBMD (it is a geometrically ergodic Markov process). Since the data are stored in a computer as a vector of locations, we can also assume that the trajectory of the process is smooth (but keeping the good properties of the RBMD), and the RBMD comes as a theoretical tool. Indeed, all the results we present remain true if we just assume that the discrete vector of locations is a geometrically ergodic Markov process in discrete time, while as suggested in Noonan et al. (2019) our model takes into account the position autocorrelation. The RBMD provides an example of a stochastic process that fulfills these conditions, and provide theoretical support for some previous results, such as those in Noonan et al. (2019).

A problem that appears in practice is that these models assume that it is possible to record the location over a long period of time to attain convergence, but battery life is an actual constraint that must be taken into account. A hands-on way researchers have found to overcome this limitation was decreasing the sampling frequency of GPS device, so the duration of the sampling gets better. The trade-off between battery life and fine-scale movement resolution is of paramount importance, as mentioned in Brown et al. (2012),

“if intervals are too long, they undersample the details of movement paths, and if too short, they oversample resting sites and deplete the unit’s battery without providing new information. We address this problem by creating a dynamic GPS schedule that is linked to the activity level of the animal via an accelerometer onboard the tracking tag.”

Brown et al. (2012, 2013) propose combining GPS information with information from an accelerometer, which automatically turns the GPS off when the animal is not moving.

So, for this purpose, several estimators have been proposed and evaluated both in empirical and simulation studies, but there has not been much about how the data were collected except the sampling frequency because of the autocorrelation introduced, as is pointed in Mitchell et al. (2019):

“Research on home-range and habitat selection for these species should therefore incorporate a consideration of how different sampling parameters and methods may affect the structure of the data and the conclusions drawn. However, factors such as these are seldom explicitly considered.”

This issue is recently faced in He et al. (2022): “using GPS devices requires making a number of decisions about sampling that can affect the robustness of a study’s conclusion”; they provide an exhaustive practitioner-oriented analysis for designing GPS-based tracking studies. It focuses on partitioning the sampling effort over time: “it can be useful to vary GPS sampling across time to focus data collection on certain time windows over others. [...] GPS devices are often switched off at night to conserve battery.” Several practical factors must be considered: because of the weight of the battery, small animals cannot be sampled for long time periods as bigger animals can be; furthermore, “battery consumption does not scale linearly with increasing sampling frequency. GPS devices use energy each time they (re)boot and search for satellites, which typically takes longer with sparser sampling regime” (He et al., 2022); there are solar-powered GPS devices that in some cases take a fixed number of days to recharge their batteries, so the sampling schedule becomes periodic (see He et al. (2022) and references therein).

So, more complex sampling schemes have been introduced in the literature but only, as far as our knowledge extends, from a practical perspective and no theoretical results support their findings. We propose a sampling method that consists of recording the position of the animal continuously, but only for certain periods of time in which the GPS is on (see Figure 1 for an example of applying this sample scheme to a simulated unidimensional trajectory). More precisely, the GPS is set alternately on during p intervals of length δ_1 , and off during $p - 1$ intervals of length δ_2 . This will be called the on-off model (see Section 3). The existence and uniqueness of such a stochastic process obtained by means of this sampling scheme is inherited from the RBMD itself. It might be considered as an intermediate solution of the trade-off explained above: it allows a higher sampling frequency but also improves the use of the battery life.

The intuition behind this is that statistical properties should not vary so much when observing the full trajectory compared to when it is observed intermittently. Our findings confirm the empirical rule (see Eq. (5) in Noonan et al. (2019)) which states that “the information content of a

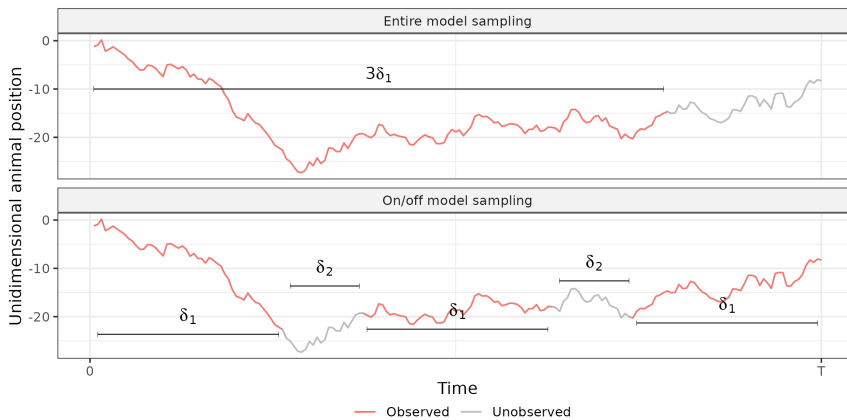


Figure 1: Top panel: in red a one dimensional process observed from time 0 to time $3\delta_1$. Bottom panel: the same process but observed intermittently, the trajectory where the GPS is on is shown in red while in grey is shown the unobserved trajectory where the GPS is off.

tracking data set is not a function of the total number of locations, [...] but rather the equivalent number of statistically independent locations”, which is usually called the effective sample size.

Assuming the RBMD underlying model, we show that any set containing the trajectory of the on–off model is a consistent estimator of S (in the Hausdorff distance) when δ_1 and δ_2 are fixed. We show that the rate of convergence of the estimator is the same as when the full trajectory is available, as $T \rightarrow \infty$ and $\delta_1 + \delta_2 \rightarrow \infty$ appropriately. The obtained rate, for $S \subset \mathbb{R}^2$, $\mathcal{O}(\log(T)^2/T)$, is close to the rate when the data is an iid sample of n points in S (which is proven to be sharp in Cuevas and Fraiman (1997)). As often happens in several nonparametric estimation problems, when we change from an iid setting to a mixing one, an extra log term appears.

Next we consider the case where the set is r -convex (see the definition in the next section) and provide consistency results with respect to the Hausdorff distance and to the distance in measure for the r -convex hull. The notion of r -convex sets has been extensively studied in various areas, particularly in stochastic geometry and set estimation, since it provides a much more general and flexible family of sets than that of convex sets, maintaining some important properties. We also provide estimators of the stationary distribution, level sets and the drift function. Lastly we provide

some simulation results and a real data example is analysed.

2. Some Preliminaries

The following notation will be used throughout this paper.

Given a set $S \subset \mathbb{R}^d$, we will denote by $\text{int}(S)$, \bar{S} and ∂S the interior, closure and boundary of S , respectively, with respect to the usual topology of \mathbb{R}^d .

The parallel set of S of radius ε will be denoted by $B(S, \varepsilon)$, that is, $B(S, \varepsilon) = \{y \in \mathbb{R}^d : \inf_{x \in S} \|y - x\| \leq \varepsilon\}$. If $A \subset \mathbb{R}^d$ is a Borel set, then $\mu(A)$ denotes its d -dimensional Lebesgue measure. We will denote by $B(x, \varepsilon)$ the closed ball in \mathbb{R}^d , of radius ε , centred at x , and $\omega_d = \mu(B(0, 1))$. The open ball is denoted by $\mathring{B}(x, \varepsilon)$. Given two compact non-empty sets $A, C \subset \mathbb{R}^d$, the Hausdorff distance between A and C is defined by

$$d_H(A, C) = \inf\{\varepsilon > 0 : \text{such that } A \subset B(C, \varepsilon) \text{ and } C \subset B(A, \varepsilon)\}.$$

Given two measurable sets $A, C \subset \mathbb{R}^d$, the distance in measure between A and C is defined by

$$d_\mu(A, C) = \mu(A \setminus C) + \mu(C \setminus A).$$

Next, we introduce the r -convex sets, a well-known shape restriction in set estimation (Walther, 1997, 1999), which extends convex sets to a much more flexible family of sets. It just replaces the hyperplanes in the definition of convex sets by the complements of balls of radius r , providing a very flexible class of sets.

Definition 2.1. A set $S \subset \mathbb{R}^d$ is said to be r -convex, for $r > 0$, if $S = C_r(S)$, where

$$C_r(S) = \bigcap_{\{\mathring{B}(x,r) : \mathring{B}(x,r) \cap S = \emptyset\}} \left(\mathring{B}(x,r)\right)^c, \quad (1)$$

is the r -convex hull of S .

Refer to Figure 2 for an example of the r -convex hull of a set of points for two different values of r .

Let us recall the definition of a C^2 boundary. Intuitively, this means that the boundary, locally, can be thought of as the graph of a C^2 function.

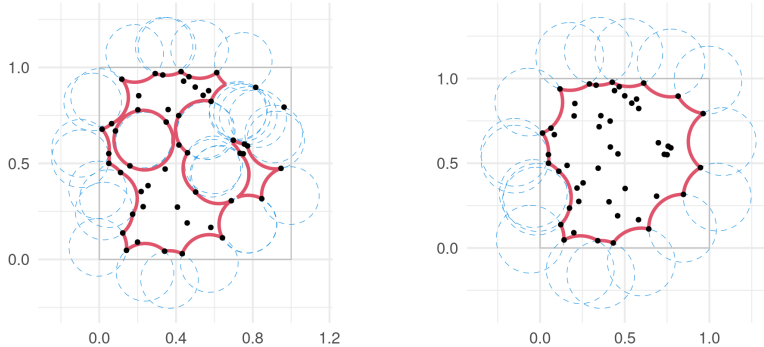


Figure 2: In solid red line the r -convex hull of a sample of 100 uniformly distributed random vectors in $[0, 1] \times [0, 1]$. At left $r = 0.15$, while at right $r = 0.2$.

Definition 2.2 (From Evans (2010)). Given a bounded set $S \subset \mathbb{R}^d$, we say that ∂S is C^2 if for every point $x \in \partial S$, there exists some real $r > 0$ and a function of class C^2 , $\gamma : \mathbb{R}^{d-1} \rightarrow \mathbb{R}$, such that –upon relabeling and reorienting axes– we have

$$S \cap B(x, r) = \{x = (x_1, \dots, x_d) \in B(x, r) : x_n > \gamma(x_1, \dots, x_{d-1})\}.$$

2.1 A brief outline of our theoretical results

We prove that any set $S_T \subset B(S, \epsilon_T)$ for $\epsilon_T \rightarrow 0$ containing the trajectory of the on–off model (that is, the times at which the GPS is on) is a consistent estimator, in the Hausdorff distance, of the home-range, and determine the improvement we can attain with the proposed new model in Theorem 3.2.

However, this is not the case if we want to estimate the set with respect to the distance in measure (w.r.t. Lebesgue measure). In this case, we propose using the r -convex hull of the same trajectory of the on–off model. When S is r -convex, a natural estimator of S from a random sample \aleph_n of points (drawn from a distribution with support S) is $C_r(\aleph_n)$, (Rodríguez Casal, 2007; Pateiro-López and Rodríguez-Casal, 2009). We show its convergence in the Hausdorff metric, while the convergence in measure is derived from Corollary 1, as mentioned in Remark 3.

In order to estimate the core-area and the drift component of the stochastic differential equation (2), we prove the uniform convergence of a kernel estimator of the stationary density, and derive estimators of the

level sets in Theorem 3.3.

An estimator of the the drift component is derived from the kernel density estimator by using Green’s formula.

Some techniques used in the proofs resemble the ones used in (Cholaquidis et al., 2016, 2021). However, the rate of convergence of the Hausdorff distance for the RBMD is not provided in the aforementioned works, nor in the literature, as far as our knowledge extends, and the behaviour of the on–off model is not considered.

2.2 Reflected Brownian motion with drift

Now we will give a brief review of the definition and main properties of the RBMD. The details can be found for instance in Cholaquidis et al. (2021) and references therein. In what follows, $S \subset \mathbb{R}^d$ is such that $S = \overline{\text{int}(S)}$ and $\text{int}(S)$ is a bounded domain in \mathbb{R}^d (that is, a bounded connected open set) such that ∂S is C^2 . Given a d -dimensional Brownian motion $\{B_t\}_{t \geq 0}$ departing from $B_0 = 0$ defined on a filtered probability space $(\Omega, \mathcal{F}, \{\mathcal{F}_t\}_{t \geq 0}, \mathbb{P})$, and a function $f : S \rightarrow \mathbb{R}$, the RBMD is the (unique) strong solution to the following reflected stochastic differential equation on S whose drift is given by the gradient of f ,

$$X_t = X_0 + B_t - \frac{1}{2} \int_0^t \nabla f(X_s) ds + \int_0^t \mathbf{n}(X_s) d\xi_s, \quad \text{where } X_t \in S, \forall t \geq 0. \tag{2}$$

Here we assume that ∇f is Lipschitz, while $\mathbf{n}(x)$ denotes the inner unit vector at the boundary point $x \in \partial S$. The term $\{\xi_t\}_{t \geq 0}$ is the corresponding *local time*, that is, a one-dimensional continuous non-decreasing process with $\xi_0 = 0$ that satisfies

$$\xi_t = \int_0^t \mathbb{I}_{\{X_s \in \partial S\}} d\xi_s,$$

see Saisho (1987). Since we have assumed that ∂S is C^2 , we can ensure that the geometric conditions for the existence of a solution of Equation (2), as required in Saisho (1987), are satisfied. We then get from Theorem 5.1 in Saisho (1987) that there exists an unique strong solution of the Skorokhod stochastic differential equation (2). The solution is a strong solution in the sense of Definition 1.6 in Ikeda and Watanabe (2014). In Cholaquidis et al. (2021) it is proved that such a set S as mentioned above is a non-trap domain for the RBMD given by (2), which is defined as follows.

Definition 2.3. We say that $\text{int}(S)$ is a *trap domain* for the stochastic process $\{Z_t\}_{t \geq 0}$ if there exists a closed ball $B \subset \text{int}(S)$ with positive radius such that $\sup_{x \in \text{int}(S)} \mathbb{E}_x[T_B] = \infty$, where $T_B = \inf\{t > 0 : Z_t \in B\}$, and \mathbb{E}_x denotes the expectation assuming $X_0 = x$ a.s. Otherwise $\text{int}(S)$ is called a *non-trap domain*.

Intuitively, the non-trap condition requires that each ball must be visited infinitely often, at an adequate rate.

The following proposition, proven in Cholaquidis et al. (2021), will be used to get the consistency in Hausdorff distance of the trajectory, as an estimator of the home-range of the on-off model.

Proposition 1. *Let $S \subset \mathbb{R}^d$ be such that $\text{int}(S)$ is a bounded domain and ∂S is C^2 . Denote by π the invariant distribution of $\{X_t\}_{t \geq 0}$. If $\text{int}(S)$ is a non-trap domain for $\{X_t\}_{t \geq 0}$, then there exist positive constants α and β such that*

$$\sup_{x \in \text{int}(S)} \|\mathbb{P}_x(X_t \in \cdot) - \pi(\cdot)\|_{TV} \leq \beta e^{-\alpha t}.$$

Here, $\|\cdot\|_{TV}$ stands for the total variation norm of a measure, and \mathbb{P}_x denotes the probability assuming $X_0 = x$ a.s.

Remark 1. *The process defined by (2) can be seen as a limit of a random walk sampling, that is, at each time we sample a point and a direction and magnitude to move. A precise proof of this is given in Burdzy and Chen (2008) and Bossy et al. (2004). This sampling scheme is used in our simulations.*

3. The On-Off Model

Our on-off model is defined as follows:

Definition 3.1. Given

- $S \subset \mathbb{R}^d$ a compact set.
- $\{X_t : t > 0\}$ a reflected Brownian motion with drift, in S .
- Two parameters $\delta_1, \delta_2 \in \mathbb{R}^+$.
- A function $\{a_t : t > 0\}$ that varies over $\{0, 1\}$ intermittently, with $a_t = 1$ for periods of length δ_1 and $a_t = 0$ for periods of length δ_2 .

More precisely,

$$a_t = \sum_{k=0}^{\infty} \mathbb{I}_{[k(\delta_1 + \delta_2), (k+1)\delta_1 + k\delta_2]}(t).$$

We define the process

$$X_T^{\text{ON}} = \{X_t : t \in \mathcal{I}, t < T\}, \quad (3)$$

where $\mathcal{I} := \{t : a_t = 1\}$. Observe that the process X_T^{ON} is defined only on a union of disjoint intervals. The function a_t works like an on–off switch: we only observe the process while $a_t = 1$ (i.e. the switch is ‘On’), which happens on intervals of length δ_1 , while it is not observable on intervals of length δ_2 , in alternation.

The following theorem provides the almost sure convergence of the Hausdorff distance between any subset of S containing the trajectory of the on–off model and the set S , when $T \rightarrow \infty$ for fixed δ_1 and δ_2 . If $\delta_1 + \delta_2 \rightarrow \infty$, the same rate of convergence is obtained as in the case where the process X_t is always observed over the whole experiment. Also, the obtained bounds are close to the rate $(n/\log(n))^{1/d}$, which was shown to be sharp in the iid case, that is, when instead of a process we have an iid sample of n points in S (see Cuevas and Fraiman (1997)).

Theorem 3.2. *Let $S \subset \mathbb{R}^d$ be a compact set such that $S = \overline{\text{int}(S)}$ and ∂S is C^2 . Let X_T^{ON} be defined as in Equation (3). Suppose that the drift is a Lipschitz function given by the gradient of some function f , and assume that the stationary distribution π has density g . Write $c := \inf_{x \in S} g(x)$.*

a) *If $\delta_1, \delta_2 > 0$ are fixed,*

$$d_H(S_T^{\text{ON}}, S) \rightarrow 0 \quad \text{a.s.} \quad (4)$$

for any set $S_T \subset S$ containing $\{X_t : t \in [0, T] \cap \mathcal{I}\}$ a.s.

b) *Let $\kappa_T = (T/\log^2(T))^{1/d}$. If*

$$\delta_1 + \delta_2 = -\frac{1}{\alpha} \log \left(\frac{\beta c}{2} \left(\frac{1}{\kappa_T \eta_T} \right)^d \right)$$

where η_T is any sequence that tends to infinity, then

$$\kappa_T d_H(S_T^{\text{ON}}, S) \rightarrow 0 \quad \text{a.s.} \quad (5)$$

for any set $S_T \subset S$ containing $\{X_t : t \in [0, T] \cap \mathcal{I}\}$ a.s.

Remark 2. *The choice of the parameters is an important practical problem. In practice, the battery life, $B = p\delta_1$, and the time T of the experiment remain fixed. Studying the optimization problem*

$$\min_{\{\delta_1, \delta_2: T=B/\delta_1+(B/\delta_1-1)\delta_2\}} d_H(S_T^{\text{ON}}, S)$$

for T and B fixed, is far beyond the scope of this paper and remains as an open problem. However, we consider different alternatives in our simulations that confirm the empirical rule known in the folklore of home-range estimation, which states that decreasing the correlation in the dataset increases the effective sample size (Noonan et al., 2019).

The following corollary is a direct consequence of Theorem 3.2, using the fact that if ∂S is C^2 , then it is r -convex for some $r > 0$, and then $C_r(X_T^{\text{ON}}) \subset S$ a.s.

Corollary 1. *Under the hypotheses of Theorem 3.2, for any measurable set S_T containing X_T^{ON} a.s., we have that, for some $r > 0$, $a_T d_H(C_r(X_T^{\text{ON}}), S) \rightarrow 0$ a.s., as $T \rightarrow \infty$, when δ_1, δ_2 are as in Theorem 3.2.*

Remark 3. *The convergence in Hausdorff distance of a sequence of r -convex sets implies the convergence of their boundaries, as is proved in Theorem 3 in Cuevas et al. (2012), which, in turn, implies the convergence in measure, i.e. $d_\mu(C_r(\mathcal{X}_T), S) \rightarrow 0$ a.s.*

3.1 Estimation of the stationary distribution, level sets, and drift

In the stochastic differential equation (2), the drift $\nu(x)$ is given by the gradient ∇f of a function f , i.e. $\nu(x) = -\frac{1}{2}\nabla f(x)$. The density of the stationary distribution (for the RBMD and the on-off process X_T^{ON}) is given by $\pi(dx) = c_0 e^{-f(x)} \mathbb{I}_D(x) dx := g(x) dx$, where c_0 is a normalization constant, as is stated in the following proposition.

Proposition 2. *Let S be such that $\text{int}(S)$ is a bounded domain and ∂S is C^2 . Assume that ∇f is Lipschitz on S . Then the measure*

$$\pi(dx) = c_0 e^{-f(x)} \mathbb{I}_{\text{int}(S)} dx \tag{6}$$

is the unique stationary measure of $\{X_t\}_{t \geq 0}$.

If $\nu = 0$, the Reflected Brownian Motion without drift is obtained and the stationary distribution is the uniform distribution in S , (Burdzy et al., 2006). The density g can also be estimated using a kernel-based estimator

$$\hat{g}_n(x) = \frac{1}{n\tau_n^d} \sum_{i=1}^n K\left(\frac{x - X_i}{\tau_n}\right) \mathbb{I}_{C_r(X_T^{\text{ON}})}(x), \quad (7)$$

where $K : \mathbb{R}^d \rightarrow \mathbb{R}$ is a non-negative function, as proved in Cholaquidis et al. (2021), based on a subsample $\aleph_n = \{X_1, \dots, X_n\}$ of points at which the GPS is on.

The a.s. uniform consistency of \hat{g}_n is stated in the following theorem.

Theorem 3.3. *Under the hypotheses of Theorem 3.2, assume further that g is Lipschitz. Let us define $\aleph_n = \{X_{(k+1)\delta_1 + k\delta_2} : k = 0, \dots, n-1\}$. Let \hat{g}_n be given by (7), based on \aleph_n . Assume that K is non-negative and Lipschitz, and that $\int K(t)dt = 1$. Let $\tau_n \rightarrow 0$ and $\gamma_n \rightarrow \infty$, such that $\gamma_n\tau_n \rightarrow 0$ and $\log(n)/\gamma_n \rightarrow 0$. Then*

$$\gamma_n \sup_{x \in S} |\hat{g}_n(x) - g(x)| \rightarrow 0 \quad \text{a.s.}$$

Moreover, if $\lambda > 0$ is such that $\partial G_g(\lambda) \neq \emptyset$, where $G_g(\lambda) = \{g > \lambda\}$, while g is C^2 on a neighbourhood E of the level set λ and the norm of the gradient of g is strictly positive on E , then $d_H(\partial G_g(\lambda), \partial G_{\hat{g}_n}(\lambda)) = o(1/\gamma_n)$ a.s.

The subsample considered in Theorem 3.3 can be replaced by any subsample $\aleph_n = \{X_{t_1}, \dots, X_{t_n}\}$ where t_i is such that the process is observed at time t_i , whenever \aleph_n is geometrically ergodic. This last condition is guaranteed for instance if there exists $\rho > 0$ (independent of n) such that for all $i = 1, \dots, n$, $t_i - t > \rho$, where t is the first observed time previous to t_i .

The level sets will provide significant information about the time spent in those regions, in particular the core-area will correspond to level sets with large values of λ .

An estimator of the drift function can also be derived from a plug-in method, and is given by $\hat{\nu}(x) = \frac{1}{2} \nabla \log(\hat{g}_n(x))$.

4. Some simulation results and an example with real data

Through some simulation examples and an example of real data, we compare the performance of the on-off model with the full model (i.e. where

the GPS is always on). To illustrate Theorem 3.2, we assume $\delta_1 = \delta_2$ in subsections 4.1 and 4.2. On the other hand, to gain some insight about some other possible choices for δ_1 and δ_2 (see Remark 3), we assume in the level-set estimation problem $\delta_1 \neq \delta_2$, see subsection 4.3. This is also the case for the example with real data, in subsection 4.4.

To simulate the RBMD, we follow Cholaquidis et al. (2021): we first choose a step $h > 0$, and denote by $\text{sym}(z)$ the point symmetric with the point z with respect to ∂S . We start with $X_0 = x$ and suppose that we have obtained $X_i \in S$. To produce the following point, set

$$Y_{i+1} = X_i + Z_i + h\nabla f(X_i),$$

where Z_i is a centred Gaussian random vector, independent of Z_1, \dots, Z_{i-1} , with covariance matrix $h \times (I_d)_{\mathbb{R}^2}$.

Then:

1. If $Y_{i+1} \in S$, set $X_{i+1} = Y_{i+1}$.
2. If $Y_{i+1} \notin S$ and $\text{sym}(Y_{i+1}) \in S$, set $X_{i+1} = \text{sym}(Y_{i+1})$.
3. If $Y_{i+1} \notin S$ and $\text{sym}(Y_{i+1}) \notin S$, set $X_{i+1} = X_i$.

Lastly, the on-off model is obtained from X_1, \dots, X_N where we only keep those X_i such that $i \in \cup_{k=0}^{\infty} \{[k(\delta_1 + \delta_2)/h, (k+1)\delta_1/h + k\delta_2/h]\}$.

We consider an RBMD in the set $S = E \setminus B((4/5, 0), 1/2)$, where $E = \{(x, y) \in \mathbb{R}^2 : 4x^2/9 + y^2 \leq 1\}$, with drift function given by $\nu(x, y) = -(x, y)$. The stationary density is

$$g(x) = c_0 e^{-(x^2+y^2)} \mathbb{1}_S(x, y) \quad \text{where } c_0^{-1} = \iint_S \exp[-(x^2 + y^2)] dx dy. \quad (8)$$

4.1 The behaviour of the Hausdorff distance

Table 1 presents the mean and the median (in parentheses), over 50 replications, of the Hausdorff distance between the set S and three competitors: the full trajectory observed on $T = p\delta_1 + (p-1)\delta_2$ (first column); the on-off model for $\delta_1 = \delta_2$ (second column); and the trajectory observed on $[0, p\delta_1]$ (third column). We choose $h = 0.0005$, $h = 0.001$, and trajectories of $N = 10^5$ steps. As can be seen, there is a performance improvement when we use the on-off model (which uses half of the battery life of the full trajectory) with respect to the process observed only on $[0, p\delta_1]$. On

h	full	on_off	$[0, p\delta_1]$
5e-04	0.2658 (0.1625)	0.2750 (0.1706)	0.4795 (0.5154)
1e-03	0.1238 (0.0785)	0.1330 (0.0871)	0.3072 (0.3128)

Table 1: Mean and median, over 50 replications, of the Hausdorff distances for the full trajectory, the on–off model, and the process observed only on $[0, p\delta_1]$, with $N = 10^5$ steps.

the other hand, the loss with respect to the full trajectory is negligible. Figure 3 shows the 50 Hausdorff distances between the trajectory of the on–off model and S (square box). Each of them is joined at its left with a segment with the corresponding red circle box (for the same trajectory), representing the Hausdorff distance between S and the full trajectory. It is also joined at its right with a segment with a green triangle representing the Hausdorff distance between S and the trajectory of the process observed only on $[0, p\delta_1]$.

4.2 The behaviour for the distance in measure

The same analysis is performed for the distance in measure. Table 2 presents the mean and the median (in parentheses), over 50 replications, of the distance in measure between the set S and three competitors: the 0.4-convex hull of the full trajectory observed on $T = p\delta_1 + (p - 1)\delta_2$ (first column), the 0.4-convex hull of the on–off model for $\delta_1 = \delta_2$ (second column), and the 0.4-convex hull of the trajectory observed on $[0, p\delta_1]$ (third column). We choose $h = 0.0005$, $h = 0.001$ and trajectories of $N = 10^5$ steps. Here again there is a performance improvement when we use the on–off model with respect to the process observed only on $[0, p\delta_1]$. Also, the loss with respect to the full trajectory is negligible. Figure 4 shows the 50 distances in measure between the trajectory of the on–off model and S (square box). As before, each of them is joined on the left with a segment with the corresponding red circle box (for the same trajectory), representing the distance in measure between S and the full trajectory. It is also joined on the right with a segment with a green triangle representing the distance in measure between S and the trajectory of the process observed only on $[0, p\delta_1]$.

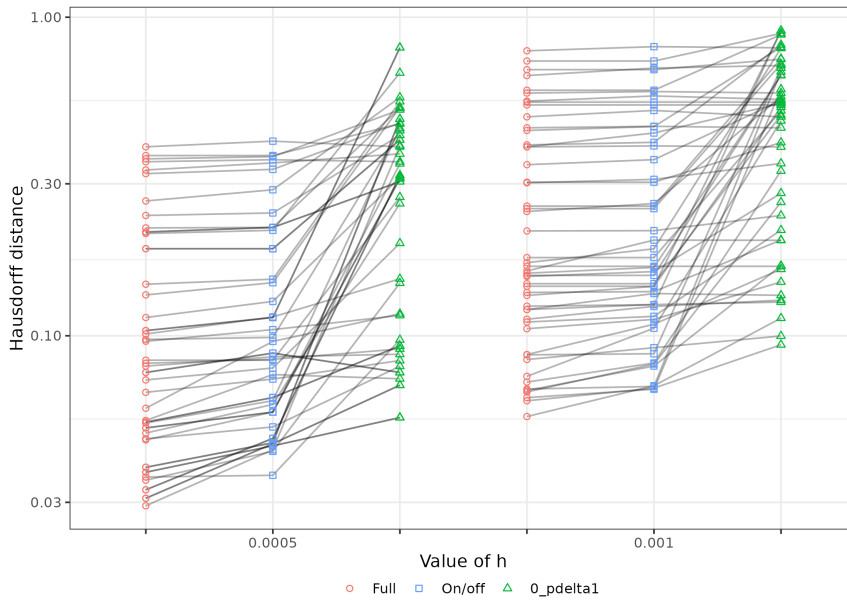


Figure 3: 50 Hausdorff distances between the trajectory of the on–off model and S (square box). Each square is joined at its left with the Hausdorff distance between S and the process always observed (red circles), and joined at its right with the Hausdorff distance between the set and the trajectory observed only on $[0, p\delta_1]$ (green triangles).

4.3 Level set estimation

Figure 5 shows the estimated level sets for two different choices of δ_1 and δ_2 , and the density g given by (8). The theoretical level sets are shown in Figure 6. The much better behaviour of the on–off model is clear when the number of points in the trajectory is small (2030 in the top panels), while the behaviour becomes similar when this number is large (98809 in the bottom panel).

The estimated density for the same set of parameters used in the first row of Figure 5 ($\delta_1 = 10$, $\delta_2 = 500$ with a total number of observations of $p\delta_1 = 2030$) is shown in Figure 7, where a Gaussian kernel with bandwidth $\tau = 0.2$ was selected by cross-validation.

h	full	on_off	$[0, p\delta_1]$
5e-04	0.1161 (0.0817)	0.1277 (0.0923)	0.3306 (0.3225)
1e-03	0.0362 (0.0119)	0.0446 (0.0220)	0.1527 (0.1468)

Table 2: Mean and median, over 50 replications, of the distance in measure for the full trajectory, the on-off model, and the process observed only on $[0, p\delta_1]$, with $N = 10^5$ steps.

4.4 An example using real data

In this section we demonstrate the performance of the on-off model using an example of real data. We consider a data set consisting of 1633 recorded positions of elephants in Loango National Park in western Gabon. The data that support the findings of this study are openly available in Movebank at https://www.movebank.org/cms/webapp?gwt_fragment=page=studies,path=study1818825, reference number 1818825. This dataset was also analysed in Cholaquidis et al. (2021). We first estimate the r -convex hull of this full trajectory. Later, we imagine that this full trajectory is not available at all, and we only have a subset of size $p\delta_1$ of the recorded locations. One approach is to observe the first $p\delta_1$ steps, and the other approach is to use our on-off strategy. Figure 8 shows, as a solid black line, the boundary of the 0.02-convex hull of the full trajectory, and the 0.02-convex hull under the two approaches. The intersection of the two is shown in green, and the differences between one and the other are shown in red and blue.

The stationary distribution is also estimated. Figure 9 presents the level set estimation for the probability density function under different choices of the parameters δ_1, δ_2 , and Figure 10 shows a three-dimensional representation of the density function for $\delta_1 = 10, \delta_2 = 100$.

5. Concluding Remarks

We obtain almost sure consistency results for the estimation under the Hausdorff distance and the distance in measure for the on-off model. We also obtain the rate of convergence for the Hausdorff distance, which turns out to be almost optimal (i.e. equal, up to a logarithmic term, to the case in which the data is an iid sample). The same rate of convergence for the Hausdorff distance is obtained if the trajectory is observed by a GPS that is always on.

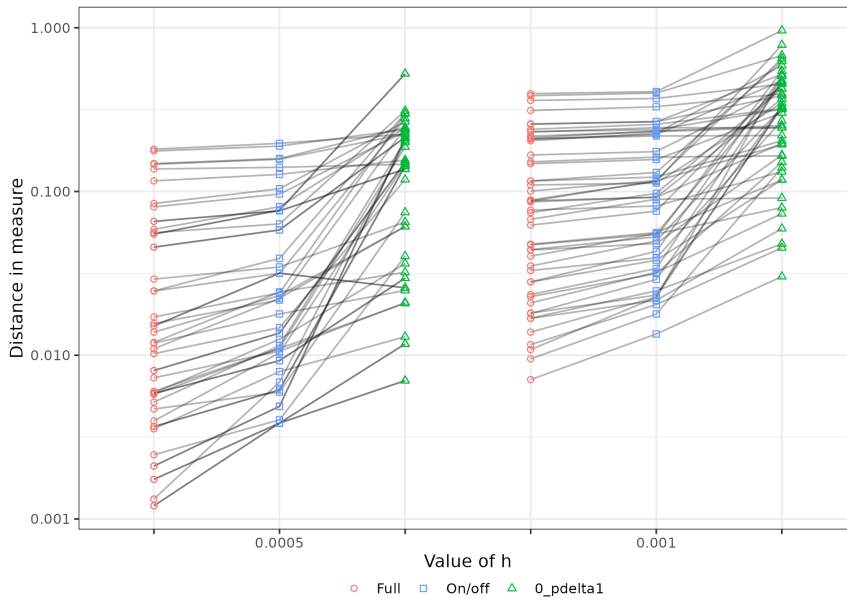


Figure 4: 50 distances in measure between the trajectory of the on–off model and S (square box). Each square is joined on its left with the distance in measure between S and the always observed process (red circles), and joined on its right with the distance in measure between the set and the trajectory observed only on $[0, p\delta_1]$ (green triangles)

The stationary distribution is estimated using a kernel type estimator as proposed in Cholaquidis et al. (2021).

From the uniform convergence of the estimated stationary distribution, we derive estimators of the level sets, which can determine the core-area of the animals’ home-range.

An estimator of the drift function can be derived from an estimator of the stationary distribution by a simple plug-in rule.

An optimal choice of the parameters δ_1, δ_2 remains an open problem; the simulations suggest that the best possible efficiency is obtained for small values of δ_1 .

It could be interesting to generalize the on–off model in future work, allowing δ_1 and δ_2 to be random variables, so the sampling scheme would also be a random variable. Such a new setup could include the case when an accelerometer governs the power status of the GPS, even also some missing

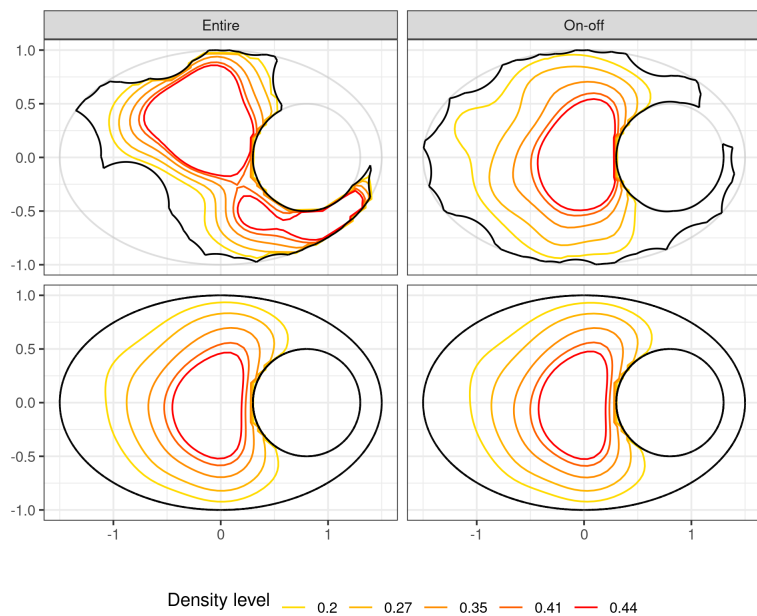


Figure 5: Top: Contour plot of the level sets of the estimated density function when $\delta_1 = 10$, $\delta_2 = 500$ with a total number of observations of $p\delta_1 = 2030$. Bottom: Contour plot of the level sets of the estimated density function when $\delta_1 = 500$, $\delta_2 = 10$ with a total number of observations of $p\delta_1 = 98809$. Left panels correspond to the entire trajectory, right panels to the on-off model.

data due to connection problems could be admitted.

Acknowledgements

We thanks Dr. Stephen Blake, of the Max Planck Institute for Ornithology, for facilitating access to the data set that was used in this paper. The data that support the findings of this study are openly available in Movebank at https://www.movebank.org/cms/webapp?gwt_fragment=page=studies,path=study1818825, reference number 1818825. This work was supported by grant FCE120191156054, ANII and POSNAC20191157608, ANII.

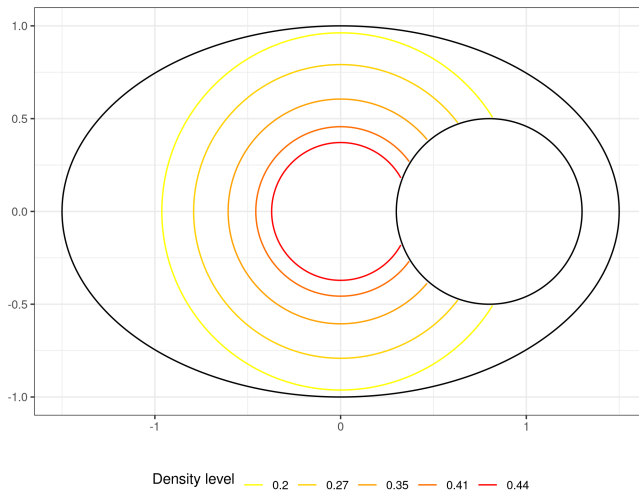


Figure 6: Theoretical level sets for the density g given by (8).

6. Appendix

6.1 Proof of Proposition 2

In order to obtain the stationary distribution, we will use the following lemma, whose proof is accomplished by reasoning as in the proof of lemma 2.1 (i) in Harrison and Williams (1987). First let us introduce some notation. We denote by $C_c^2(S)$ the set of twice continuously differentiable functions with compact support in some domain containing S . We write \mathcal{L} for the infinitesimal generator of the process, i.e. $\mathcal{L}(h)(x) = \lim_{t \downarrow 0} (1/t)(\mathbb{E}_x(h(X_t)) - h(x))$. It can be proved that $\mathcal{L}h = \frac{1}{2}\Delta h - \frac{1}{2}\langle \nabla f, \nabla h \rangle$, for $h \in C_c^2(S)$, (Cholaquidis et al., 2021).

Lemma 6.1. *Let S satisfy $S = \overline{\text{int}(S)}$, and suppose $\text{int}(S)$ is a bounded domain and ∂S is C^2 . Suppose that $p: S \rightarrow \mathbb{R}$ is C^2 , positive on $\text{int}(S)$, and that $\int_{\text{int}(S)} p(x)dx = 1$. Then p is the density of the (unique) invariant distribution for (2) if and only if*

$$\int_{\text{int}(S)} p(x)\mathcal{L}h(x)dx = 0 \quad \text{for all } h \in C_c^2(S) \text{ satisfying } \langle \nabla h(x), \mathbf{n}(x) \rangle = 0 \text{ on } \partial S, \quad (9)$$

where $\mathbf{n}(x)$ denotes the inner normal vector at $x \in \partial S$.

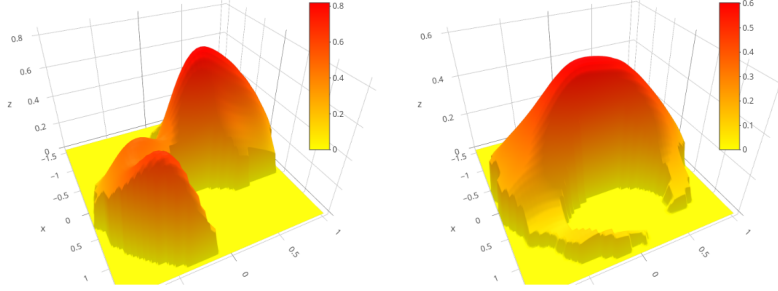


Figure 7: Estimated density using a Gaussian kernel with bandwidth $\tau = 0.2$. Right: the on–off model with $\delta_1 = 10$, $\delta_2 = 500$ with a total number of observations of $p\delta_1 = 2030$. Left: Estimated density based on trajectory observed with same number of observations but on $[0, 2030]$.

Proof of Proposition 2

By Lemma 6.1, the measure π is the stationary distribution if and only for all $h \in C_c^2(S)$ with $\langle \mathbf{n}(x), \nabla h(x) \rangle = 0$, for all $x \in \partial S$, one has that $0 = \int_{\text{int}(S)} c e^{-f(x)} \mathcal{L}h(x) dx$. But this is a direct consequence of Green’s first identity:

$$\begin{aligned} - \int_{\text{int}(S)} e^{-f(x)} \Delta h(x) dx &= \int_{\partial S} e^{-f(x)} \langle \nabla h(x), \mathbf{n}(x) \rangle d\sigma(x) + \int_{\text{int}(S)} e^{-f(x)} \langle \nabla f(x), \nabla h(x) \rangle dx \\ &= \int_{\text{int}(S)} e^{-f(x)} \langle \nabla f(x), \nabla h(x) \rangle dx, \end{aligned}$$

with σ being the surface measure on ∂S .

6.2 Proof of Theorem 3.2 a)

Assume first that δ_1 and δ_2 are positive and fixed. Let us fix $\epsilon > 0$. We will define a grid depending on ϵ , on $[0, T] \cap \mathcal{I}$. Let us define $t_\epsilon := -(1/\alpha) \log(\beta c(\epsilon/2)^d/2)$. Let us define $t_i := i \times s(\delta_1 + \delta_2)$ for $i \in \mathbb{N}$, where s is the smallest integer that guarantees $s(\delta_1 + \delta_2) > t_\epsilon$. Then, for all n , there exists T large enough, such that there exist $t_1, \dots, t_n \in \mathcal{I} \cap [0, T]$ and $t_{i+1} - t_i > t_\epsilon$ for all $i = 1, \dots, n - 1$.

We will assume that the process is ON in $[T - \delta_1, T]$.

Denote the ϵ –inner parallel set of S by

$$S^{(\epsilon)} = \{x \in S : B(x, \epsilon) \subset S\}.$$

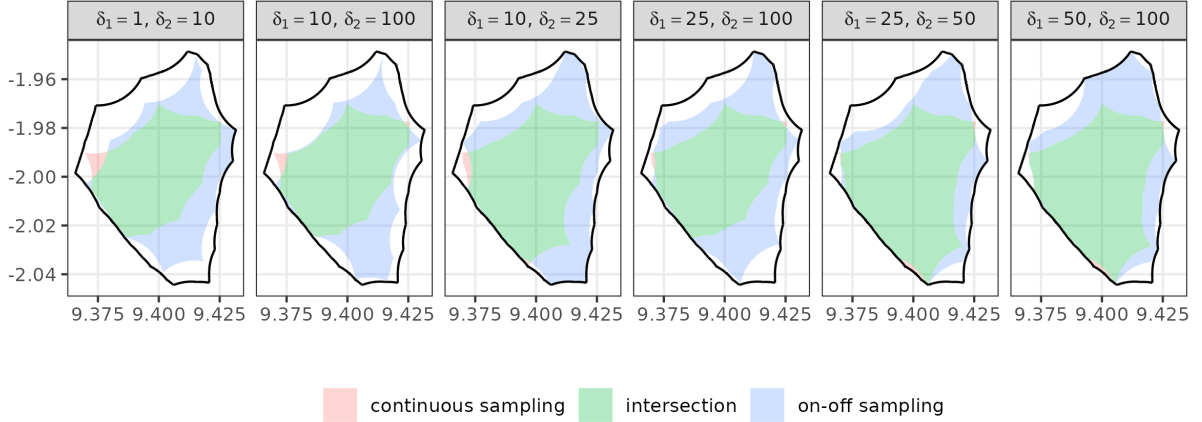


Figure 8: Each panel shows, for different values of δ_1 and δ_2 , the 0.02-convex hull of the trajectory observed under the on–off model compared with the 0.02-convex hull of that observed without interruption for the same length of time. The intersection of both sets is shown in green, and the differences are shown in red and blue. In black solid line, the boundary of the 0.02-convex hull of the whole trajectory available.

Put $I_n := \{1, \dots, n\} \cap \{i : a_{t_i} = 1\}$, the indices at which the process is observed. Then

$$\begin{aligned} \mathbb{P}\{d_H(S_T^{\text{ON}}, S) > \varepsilon\} &\leq \mathbb{P}\{\exists x \in S^{(\varepsilon)} : \forall t \in \mathcal{I}, t < T : X_t \notin B(x, \varepsilon)\} \\ &\leq \mathbb{P}\{\exists x \in S^{(\varepsilon)} : \forall i \in I_n : X_{t_i} \notin B(x, \varepsilon)\}. \end{aligned}$$

Let $x_1, \dots, x_N \in S^{(\varepsilon)}$ be such that $S^{(\varepsilon)} \subset B(x_1, \varepsilon/2) \cup \dots \cup B(x_N, \varepsilon/2)$, and suppose that N is the smallest positive integer such that such a covering of $S^{(\varepsilon)}$ is possible. Then $N = N(\varepsilon/2)$ is called the $\varepsilon/2$ -covering number of $S^{(\varepsilon)}$. It is easy to see (and well known) that $N \leq \mu(S)/\mu(B(0, \varepsilon/4)) = (\varepsilon/4)^{-d} \mu(S)/\omega_d$.

If for some $x \in S$ we have $X_{t_i} \notin B(x, \varepsilon)$ for all $i \in I_n$, then there exists a $j \in \{1, \dots, N\}$ such that $X_{t_i} \notin B(x_j, \varepsilon/2)$ for all $i = 1, \dots, n$. Thus, continuing the chain of inequalities above,

$$\begin{aligned} \mathbb{P}\{d_H(S_T^{\text{ON}}, S) > \varepsilon\} &\leq \mathbb{P}\{\exists j \in \{1, \dots, N\} : \forall i \in I_n : X_{t_i} \notin B(x_j, \varepsilon/2)\} \\ &\leq N \sup_{x \in S^{(\varepsilon)}} \mathbb{P}\{\forall i \in I_n : X_{t_i} \notin B(x, \varepsilon/2)\}. \end{aligned}$$

Next we estimate the probability on the right-hand side. Recall that the process is ON in $[T - \delta_1, T]$, and so $n \in I_n$. For all $x \in S^{(\varepsilon)}$,

$$\begin{aligned}
& \mathbb{P}\{\forall i \in I_n : X_{t_i} \notin B(x, \varepsilon/2)\} \\
&= \mathbb{P}\{X_{t_n} \notin B(x, \varepsilon/2) | \forall i \in I_{n-1} : X_{t_i} \notin B(x, \varepsilon/2)\} \\
&\quad \times \mathbb{P}\{\forall i \in I_{n-1} : X_{t_i} \notin B(x, \varepsilon/2)\} \\
&= \mathbb{P}\{X_{t_n} \notin B(x, \varepsilon/2) | X_{t_{n-1}} \notin B(x, \varepsilon/2)\} \\
&\quad \times \mathbb{P}\{\forall i \in I_{n-1} : X_{t_i} \notin B(x, \varepsilon/2)\} \\
&\quad \text{(since } X_t \text{ is a Markov process)}
\end{aligned}$$

Denote by π the invariant distribution of the process $\{X_t^{ON}\}_{t>0}$. Let us iterate this process

$$\mathbb{P}\{\forall i \in I_n : X_{t_i} \notin B(x, \varepsilon/2)\} = \prod_{i=0}^{n-1} \mathbb{P}\{X_{t_{n-i}} \notin B(x, \varepsilon/2) | X_{t_{n-i-1}} \notin B(x, \varepsilon/2)\}.$$

Now, by Proposition 1,

$$\begin{aligned}
& \mathbb{P}\{X_{t_{n-i}} \notin B(x, \varepsilon/2) | X_{t_{n-i-1}} \notin B(x, \varepsilon/2)\} = \\
&\quad 1 - \mathbb{P}\{X_{t_{n-i}} \in B(x, \varepsilon/2) | X_{t_{n-i-1}} \notin B(x, \varepsilon/2)\} \\
&\quad \leq 1 - \pi(B(x, \varepsilon/2)) + \beta \exp\{-\alpha(t_{n-i} - t_{n-i-1})\} \\
&\quad = 1 - c\omega_d \varepsilon^d / 2^{d+1}. \tag{10}
\end{aligned}$$

$$\prod_{i=0}^{n-1} \mathbb{P}\left\{X_{t_{n-i}} \notin B(x, \varepsilon/2) | X_{t_{n-i-1}} \notin B(x, \varepsilon/2)\right\} \leq \left(1 - \frac{c\omega_d \varepsilon^d}{2^{d+1}}\right)^n \leq \exp\left(\frac{-nc\omega_d \varepsilon^d}{2^{d+1}}\right)$$

Then

$$\mathbb{P}\{d_H(S_T^{ON}, S) > \varepsilon\} \leq \frac{(\varepsilon/4)^{-d} \mu(S)}{\omega_d} \exp\left(\frac{-nc\omega_d \varepsilon^d}{2^{d+1}}\right).$$

From the Borel–Cantelli Lemma, there follows a).

6.3 Proof of Theorem 3.2 b)

The proof follows the same ideas used to prove part a). Fix $\varepsilon > 0$. We will define a grid depending on ε and T , on $[0, T] \cap \mathcal{I}$. Let us define, for $i \in \mathbb{N}$, $t_i = i \times (\delta_1 + \delta_2)$. We will assume that the process is ON in $[T - \delta_1, T]$. Proceeding as in (10),

$$\begin{aligned}
\mathbb{P}\{X_{t_{n-i}} \notin B(x, \varepsilon/(2\kappa_T)) | X_{t_{n-i-1}} \notin B(x, \varepsilon/(2\kappa_T))\} &= \\
&= 1 - \mathbb{P}\{X_{t_{n-i}} \in B(x, \varepsilon/(2\kappa_T)) | X_{t_{n-i-1}} \notin B(x, \varepsilon/(2\kappa_T))\} \\
&\leq 1 - \pi(B(x, \varepsilon/(2\kappa_T))) + \beta \exp\{-\alpha(\delta_1 + \delta_2)\} \\
&\leq 1 - c\varepsilon^d/(2\kappa_T)^d + \beta \exp\{-\alpha(\delta_1 + \delta_2)\}.
\end{aligned}$$

Since $\eta_T \rightarrow \infty$, for all ε there exists T large enough such that

$$\beta \exp\{-\alpha(\delta_1 + \delta_2)\} \leq c\varepsilon^d/(2^{d+1}\kappa_T^d).$$

Since $n = \lfloor T/(\delta_1 + \delta_2) \rfloor$, we get

$$\begin{aligned}
\prod_{i=0}^{n-1} \mathbb{P}\left\{X_{t_{n-i}} \notin B(x, \varepsilon/(2\kappa_T)) | X_{t_{n-i-1}} \notin B(x, \varepsilon/(2\kappa_T))\right\} &\leq \\
&\leq \left(1 - \frac{c\omega_d\varepsilon^d}{2^{d+1}\kappa_T^d}\right)^{T/[\delta_1+\delta_2]} \leq \exp\left(-\frac{Tc\omega_d\varepsilon^d}{2^{d+1}\kappa_T^d}\right).
\end{aligned}$$

Lastly, part b) follows from the Borel–Cantelli Lemma using the fact that $\kappa_T = (T/\log^2(T))^{1/d}$.

6.4 Proof of Theorem 3.3

It is easy to prove, following the ideas used to prove Proposition 2 in Cholaquidis et al. (2021), that the chain \mathfrak{N}_n is geometrically ergodic. Then $\gamma_n \sup_{x \in S} |\hat{g}_n(x) - g(x)| \rightarrow 0$ a.s. follows as a direct application of Theorem 1 in Cholaquidis et al. (2021). From Corollary 1 together with Remark 4 in Cholaquidis et al. (2021) it follows that $d_H(\partial G_g(\lambda), \partial G_{\hat{g}_n}(\lambda)) = o(1/\gamma_n)$ a.s.

References

Bossy, M., Gobet, E., and Talay, D. (2004). ‘A symmetrized euler scheme for an efficient approximation of reflected diffusions.’ *Journal of applied probability*, 41(3):877–889.

- Brown, D. D., Kays, R., Wikelski, M., Wilson, R., and Klimley, A. P. (2013). ‘Observing the unwatchable through acceleration logging of animal behavior.’ *Animal Biotelemetry*, 1(1):1–16.
- Brown, D. D., LaPoint, S., Kays, R., Heidrich, W., Kümmeth, F., and Wikelski, M. (2012). ‘Accelerometer-informed gps telemetry: Reducing the trade-off between resolution and longevity.’ *Wildlife Society Bulletin*, 36(1):139–146.
- Burdzy, K. and Chen, Z.-Q. (2008). ‘Discrete approximations to reflected brownian motion.’ *The Annals of Probability*, 36(2):698–727.
- Burdzy, K., Chen, Z.-Q., and Marshall, D. E. (2006). ‘Traps for reflected brownian motion.’ *Mathematische Zeitschrift*, 252(1):103–132.
- Burgman, M. A. and Fox, J. C. (2003). ‘Bias in species range estimates from minimum convex polygons: implications for conservation and options for improved planning.’ *Animal Conservation Forum*, 6, 19–28. University Press.
- Burt, W. H. (1943). ‘Territoriality and home range concepts as applied to mammals.’ *Journal of mammalogy*, 24(3):346–352.
- Calabrese, J. M., Fleming, C. H., and Gurarie, E. (2016). ‘ctmm: an r package for analyzing animal relocation data as a continuous-time stochastic process.’ *Methods in Ecology and Evolution*, 7(9):1124–1132.
- Cholaquidis, A., Fraiman, R., Lugosi, G., and Pateiro-López, B. (2016). ‘Set estimation from reflected brownian motion.’ *Journal of the Royal Statistical Society: Series B (Statistical Methodology)*, 78(5):1057–1078.
- Cholaquidis, A., Fraiman, R., Mordecki, E., and Papalardo, C. (2021). ‘Level set and drift estimation from a reflected brownian motion with drift.’ *Statistica Sinica*, 31:29–51.
- Cuevas, A. and Fraiman, R. (1997). ‘A plug-in approach to support estimation.’ *The Annals of Statistics*, pages 2300–2312.
- Cuevas, A., Fraiman, R., and Pateiro-López, B. (2012). ‘On statistical properties of sets fulfilling rolling-type conditions.’ *Advances in Applied Probability*, 44(2):311–329.

- Evans, L. C. (2010). *Partial differential equations*, volume 19. ‘American Mathematical Soc.’
- Fleming, C. H., Calabrese, J. M., Mueller, T., Olson, K. A., Leimgruber, P., and Fagan, W. F. (2014). ‘From fine-scale foraging to home ranges: a semivariance approach to identifying movement modes across spatiotemporal scales.’ *The American Naturalist*, 183(5):E154–E167.
- Fleming, C. H., Fagan, W. F., Mueller, T., Olson, K. A., Leimgruber, P., and Calabrese, J. M. (2015). ‘Rigorous home range estimation with movement data: a new autocorrelated kernel density estimator.’ *Ecology*, 96(5):1182–1188.
- Getz, W. M. and Wilmers, C. C. (2004). ‘A local nearest-neighbor convex-hull construction of home ranges and utilization distributions.’ *Ecography*, 27(4):489–505.
- Harrison, J. M. and Williams, R. J. (1987). ‘Multidimensional reflected brownian motions having exponential stationary distributions.’ *The Annals of Probability*, pages 115–137.
- Hayne, D. W. (1949). ‘Calculation of size of home range.’ *Journal of mammalogy*, 30(1):1–18.
- He, P., Klarevas-Irby, J. A., Papageorgiou, D., Christensen, C., Strauss, E. D., and Farine, D. R. (2022). ‘A guide to sampling design for gps-based studies of animal societies.’ *Methods in Ecology and Evolution*.
- Horne, J. S., Garton, E. O., Krone, S. M., and Lewis, J. S. (2007). ‘Analyzing animal movements using brownian bridges.’ *Ecology*, 88(9):2354–2363.
- Ikeda, N. and Watanabe, S. (2014). *Stochastic differential equations and diffusion processes*. ‘Elsevier.’
- Kie, J. G., Matthiopoulos, J., Fieberg, J., Powell, R. A., Cagnacci, F., Mitchell, M. S., Gaillard, J.-M., and Moorcroft, P. R. (2010). ‘The home-range concept: are traditional estimators still relevant’ with modern telemetry technology?’ *Philosophical Transactions of the Royal Society B: Biological Sciences*, 365(1550):2221–2231.

- Mitchell, L. J., White, P. C., and Arnold, K. E. (2019). ‘The trade-off between fix rate and tracking duration on estimates of home range size and habitat selection for small vertebrates.’ *PloS one*, 14(7):e0219357.
- Noonan, M. J., Tucker, M. A., Fleming, C. H., Akre, T. S., Alberts, S. C., Ali, A. H., Altmann, J., Antunes, P. C., Belant, J. L., Beyer, D., et al. (2019). ‘A comprehensive analysis of autocorrelation and bias in home range estimation.’ *Ecological Monographs*, 89(2):e01344.
- Pateiro-López, B. and Rodríguez-Casal, A. (2009). ‘Surface area estimation under convexity type assumptions.’ *Journal of Nonparametric Statistics*, 21(6):729–741.
- Powell, R. A. (2000). ‘Animal home ranges and territories and home range estimators.’ *Research techniques in animal ecology: controversies and consequences*, 442:65–110.
- Rodríguez Casal, A. (2007). ‘Set estimation under convexity type assumptions.’ *Annales de l’IHP Probabilités et statistiques*, 43: 763–774.
- Saisho, Y. (1987). ‘Stochastic differential equations for multi-dimensional domain with reflecting boundary.’ *Probability Theory and Related Fields*, 74(3):455–477.
- Walther, G. (1997). ‘Granulometric smoothing.’ *The Annals of Statistics*, pages 2273–2299.
- Walther, G. (1999). ‘On a generalization of blaschke’s rolling theorem and the smoothing of surfaces.’ *Mathematical methods in the applied sciences*, 22(4):301–316.
- Worton, B. (1987). ‘A review of models of home range for animal movement.’ *Ecological modelling*, 38(3-4):277–298.

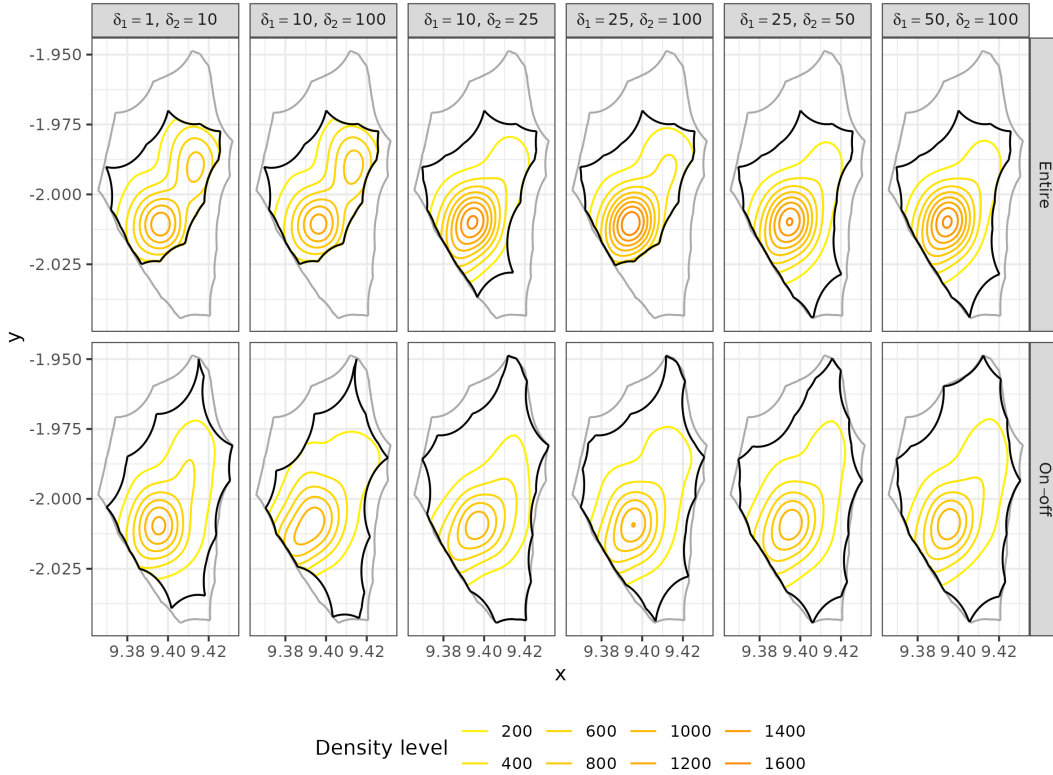


Figure 9: Contour plot of the level sets of the estimated density function for different choices of δ_1 and δ_2 . Top: cases when the trajectory is observed without interruption. Bottom: cases when the trajectory is observed under the on-off model. A Gaussian kernel was used with bandwidth parameter $\tau = 0.028$.

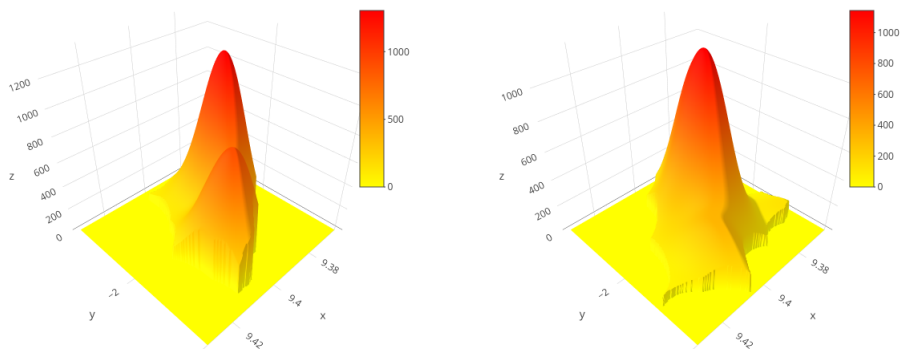


Figure 10: Estimated density using a Gaussian kernel with bandwidth $\tau = 0.028$. Right: the on-off model with $\delta_1 = 10$, $\delta_2 = 100$ with 140 observations. Left: Estimated density based on first 140 observations of the trajectory (same number of observations).